Improved Design of Subcritical and Supercritical Cascades Using Complex Characteristics and Boundary-Layer Correction

Jose M. Sanz*
Universities Space Research Association, Columbia, Maryland

The method of complex characteristics and hodograph transformation for the design of shockless airfoils was introduced by Bauer, Garabedian, and Korn and has been extended here to the design of supercritical cascades with high solidities and large inlet angles. This new capability was achieved by introducing a new conformal mapping of the hodograph domain onto an ellipse and expanding the solution in terms of Tchebycheff polynomials. A new computer code was developed based on this idea. In this paper, a number of airfoils designed with the new code are presented. Various supercritical and subcritical compressor, turbine, and propeller sections are shown. The lag-entrainment method of Green, Weeks, and Brooman for the calculation of a turbulent boundary layer has been incorporated into the inviscid design code. The results of these calculations are shown for the airfoils described in the paper. The elliptic conformal transformation developed to map the hodograph domain onto an ellipse can be used to generate a conformal grid in the physical domain of a cascade of airfoils with open trailing edges in a single transformation. A grid generated with this transformation is shown for the Korn airfoil.

I. Introduction

THE method of complex characteristics and hodograph transformation for the design of shockless airfoils was introduced by Bauer et al.,[1] and has been extended by the author[2] to design supercritical cascades with high solidities and large inlet angles. This new capability was achieved by introducing a new conformal mapping of the hodograph domain onto an ellipse and expanding the solution in terms of Tchebycheff polynomials. A new computer code was developed based on this idea.

The design of two-dimensional inviscid subcritical and supercritical cascades has been widely accepted as a method to produce axial compressor and turbine blades. With this method, a number of sections spanning from hub to tip can be designed independently of each other and according to the flow conditions required in the spanwise direction. Five of these two-dimensional sections are usually enough to design a blade with considerable three-dimensional effects.

In this design procedure the basic two-dimensional (2-d) code has to be able to handle high solidities, usually at the hub sections, and high stagger or inlet angles at the tip sections, especially in compressor rotors. Low maximum thickness-to-chord ratios are desirable for compressor blades. For turbine blades, large turning angles exceeding 100 deg will not be unusual and thick blades, in general, will be required for cooling purposes. In this case thick trailing edges will be necessary.

In Secs. II and III of this paper we review the method and report some improved new designs of compressor and turbine blades. A midspan propeller section is also shown. Although the primary purpose of the new code is the design of supercritical cascades, emphasis is made on the design of subcritical cascades because of the robustness of the code in this type of design as well as the low CPU time and overall time necessary to achieve a good design.

Section IV describes the results obtained with the incorporation of a turbulent boundary-layer computation to the inviscid design code. The lag-entrainment method of Green et al.[3] has been incorporated into the code. Since the inverse design code uses an input surface pressure distribution, it is especially well suited for this coupling. An inviscid blade is first designed with the approximate required inlet angle and Mach number, turning, and solidity. The turbulent boundary-layer computation is then switched on, and by modification of the input pressure distribution, the required design conditions are obtained, ensuring that no separation occurs.

The last section describes a cascade grid generator based on the same elliptic transformation that the author has introduced for the inverse hodograph method. A single conformal transformation suffices to map a cascade plane onto the computational domain. Open trailing edges can be handle with this transformation. A grid generated with this procedure is shown for the Korn airfoil.

II. Review of the Method

A complete description of the complex characteristic design method can be found in Ref. 1, and the elliptic hodograph transformation and new code are described in Ref. 2. We briefly review the design method. The basic idea is to construct, by numerical integration, and analytic solution to the potential flow equations finding, along with this solution, the body that corresponds to a prescribed surface pressure distribution. The equations of potential flow can be written in the hodograph complex characteristics form:

$$\varphi_\xi = \tau + \psi_\xi \qquad \varphi_\eta = \tau_- \psi_\eta$$

$$\tau_\pm = \pm i\sqrt{1-M^2}/\rho \tag{1}$$

where φ and ψ are the potential and stream functions, and M and ρ are the Mach number and density. The complex characteristics coordinates ξ and η are defined by means of the conformal transformations

$$f(\xi) = \log h - i\theta \qquad \overline{f(\bar{\eta})} = \log h + i\theta$$

$$\frac{dh}{h} = \sqrt{1-M^2}\,\frac{dq}{q} \tag{2}$$

Presented at the Sixth International Symposium on Air Breathing Engines, Paris, France, June 6-11, 1983, received July 8, 1983, revision received Nov. 17, 1983.

*Research Scientist; presently at NASA Lewis Research Center, Fluid Mechanics and Acoustics Division, Computational Fluid Mechanics Branch, Cleveland, Ohio. Member AIAA.

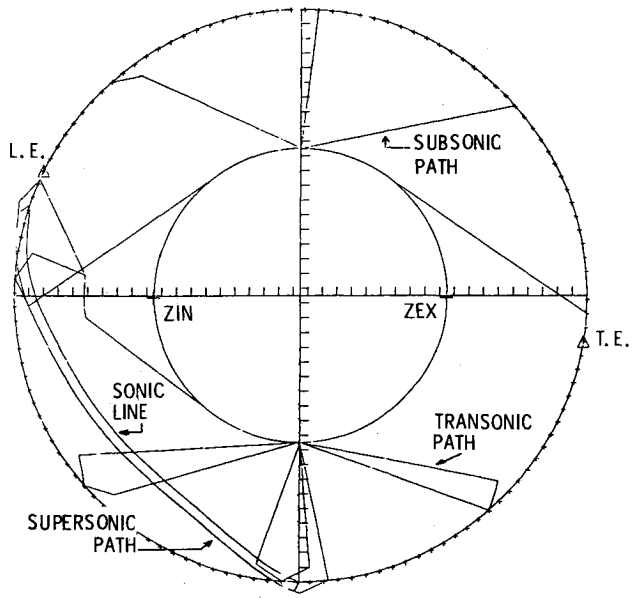

Fig. 1 Hodograph plane.

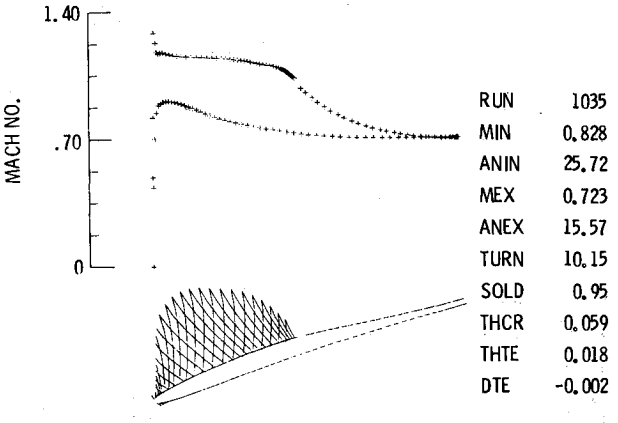

Fig. 2 Supercritical propeller section. Mach No. distribution.

and where h and θ are the Chaplygin hodograph variables and q is the modulus of the velocity vector. The characteristic coordinate ξ, and similary η, is defined in a circular ring $1 \leq |\xi| \leq R$. The conformal transformation

$$w = \frac{1}{2}\left(\xi + \frac{1}{\xi}\right), \qquad 1 \leq |\xi| \leq R \tag{3}$$

maps this circular ring onto an ellipse. Any analytic function on the ellipse can be expanded in the form:

$$f(w) = \sum_{0}^{\infty} c_n T_n(w) = c_0' + \sum_{1}^{\infty} c_n' \left(\xi^n + \frac{1}{\xi^n}\right) \tag{4}$$

where

$$T_n(w) = \frac{1}{2^n}\left(\xi^n + \frac{1}{\xi^n}\right), \qquad n = 1,2,\ldots \tag{5}$$

are the Tchebicheff polynomials.[2]

Because Eqs. (1) are linear in a hodograph domain, a complete set of solutions can be found by solving the characteristic initial value problem

$$\psi(\xi,0) = g(\xi) = \overline{\psi(0,\ \bar{\xi})} \tag{6}$$

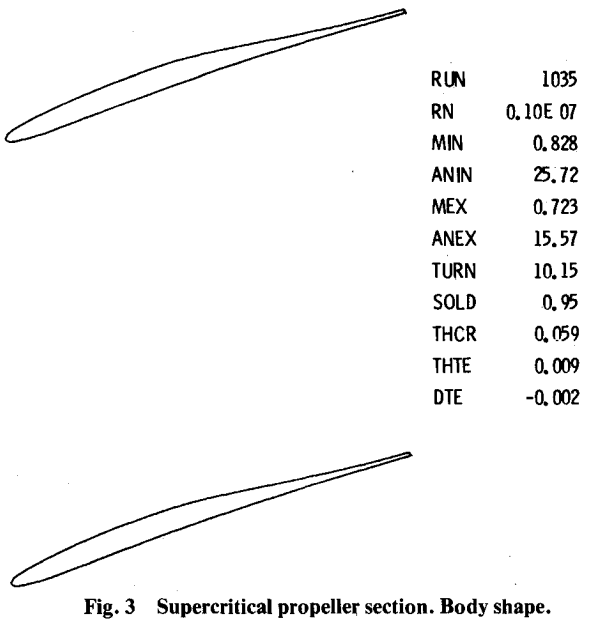

Fig. 3 Supercritical propeller section. Body shape.

where the regular part of the characteristic initial value function g can be expanded in terms of the Tchebycheff polynomials. The coefficients of that expansion can be determined by imposing the boundary-value problem

$$R_e\{\psi(\xi,\bar{\xi})\} = 0 \tag{7}$$

This characteristic initial value problem can be solved when the mapping function f is known, since the coefficients $\tau_{\pm}$ depend on it implicitly. On the other hand, the mapping function f is determined by the Dirichlet problem

$$R_e\{f(\xi)\} = \log h^* \tag{8}$$

where h^* is based on the prescribed input speed distribution. Equations (7) and (8) can be solved by means of an iterative process.[1,2]

The use of complex characteristics allows extension of the computation to mixed flows. Although the equations are established in the four-dimensional space of two complex variables, the computation is carried out in a two-dimensional manifold, conformally transformed from a two-dimensional rectangular computational domain. The topology of this manifold is such that it avoids the sonic surface where the equations of the flow become ill-conditioned.

The computation is started at a subsonic point and is continued through the complex domain until it reaches the real supersonic region without intersecting the sonic surface. In the supersonic region it first reaches the body surface and then the sonic line. This technique avoids the inaccuracies that the ill conditioning of the equations near the sonic line could introduce. The elliptic transformation, by restricting the position of the upstream and downstream points of infinity to the foci of the ellipse, makes it possible to simplify the topology of these paths of integration. For purely subsonic flows, the two-dimensional manifold, where the solution is carried out, becomes the "diagonal" of the four-dimensional space, simplifying and reducing the computation.

III. Subsonic and Supersonic Design

A wide variety of airfoils in cascade now can be designed with this inverse design procedure. The input to the design code can be separated into three parts. First we specify a surface speed distribution. By means of this input speed distribution we control the aerodynamic performance on the airfoil.

Second, three design parameters must be given. These parameters are the radius R of the outer circumference of the circular ring in the hodograph domain which controls the solidity of the cascade; the angle θ which locates the leading-edge stagnation point, and thereby controls the stagger angel; and a Mach parameter controlling the inlet Mach number.

The third set of parameters, or numerical parameters, is concerned with the accuracy vs computational speed of the design process. The parameters are: grid size for the subsonic or supersonic region, number of Fourier coefficients for the mapping function, number of iterations, etc.

To achieve a good design one could proceed in the following way. An input speed distribution is prescribed that reflects the desired aerodynamic behavior. Then the three design parameters are determined. The parameter R, which controls the solidity, can be chosen with values that, in practical terms, vary from 1.4 for a solidity of approximately 2 to a value of 2.5 for lower solidities of about 1. In the same manner we set θ for the leading-edge stagnation point and the input Mach number.

A run can be made with this set of input parameters, and the design parameters changed successively until the inlet flow conditions and solidity are obtained. The advantage of the elliptic transformation is that changes in each of the three parameters have little effect on the flow variables that the two other parameters control. For instance, large changes in θ have small effects on the solidity.

Once the required solidity, inlet Mach number, and inlet air angle are obtained, the input speed distribution is modified. This modification increases or decreases the lift, and thus the turning angle of the blade, by changing the area enclosed by the speed distribution. When the required turning has been achieved, and hence the exit flow conditions, the input speed distribution is used to tailor the body geometry. The maximum thickness of the airfoil, the leading-edge curvature, and the trailing-edge thickness can then be adjusted.

If all of the numerical parameters are kept at their default values, a subcritical airfoil can be designed with as little as 30 s of CPU time per run on an IBM 370-3033 at the NASA Lewis Research Center. Subcritical designs can be obtained with as few as 15 runs, including the boundary-layer correction. This makes the design of subcritical airfoils a very fast and reliable process.

For transonic designs the situation is more complicated. First, we do not know if a shock-free solution exists in the region we are searching. The paths of integration, although automated not to intersect the sonic line, can reach an incorrect branch of the analytic solution. Also, limit lines can appear in the supersonic region. The number of points in the computational domain is much larger, both because the integration paths are longer and because a finer grid is required, increasing the CPU time considerably. The procedure for a transonic design would be to obtain first a subsonic blade with flow characteristics close to the design in question. Then, raising the input Mach number a supersonic region will be formed and the design parameters tuned to obtain the desired blade. In the final stages, a transonic run with a fine grid and a Richardson extrapolation in both the subsonic and supersonic regions takes about 5 min of CPU time on the IBM 370-3033.

In the rest of this section six airfoils designed with this precedure are described. The first one is a transonic airfoil fit for a midspan section of a modern propeller. An inlet Mach number of 0.83 was reached before the appearance of limiting lines. The maximum thickness to chord ratio of 0.059 is reached at about 45% of the chord, which makes it an attractive design. Figure 1 shows a hodograph plane for this airfoil. In Fig. 2 can be seen the surface Mach number distribution obtianed and the inviscid airfoil. Figure 3 shows the relative position of the airfoils in the cascade plane. A cubic spline has been passed through the airfoil after subtracting the computed displacement thickness.

The next airfoil, Figs. 4 and 5, represents a tip section for a compressor rotor. The inlet Mach number reached is 0.86. This airfoil shows a large supersonic region on the suction side and an incipient supersonic bubble on the pressure side. The thickness-to-chord ratio at the trailing edge is 0.024, after subtracting the displacement thickness. Next, a low-speed rotor tip section with a high inlet air angle of 71 deg is shown in Figs. 6 and 7.

The code has been used to design two turbine blade sections shown in Figs.8-11. The first one is a subcritical section with a solidity of 1.77 (gap-to-chord ratio of 0.56). The surface speed distribution presents an accelerated profile on both sides of the blade. A small amount of diffusion is present in the last 30% of the suction side to obtain the correct trailing-edge opening. This airfoil has been designed to form the midspan section of a cooled turbine rotor.

After this subcritical design, a supercritical turbine blade section is shown with half the solidity of the previous design, and the same flow turning. This naturally implies that one-

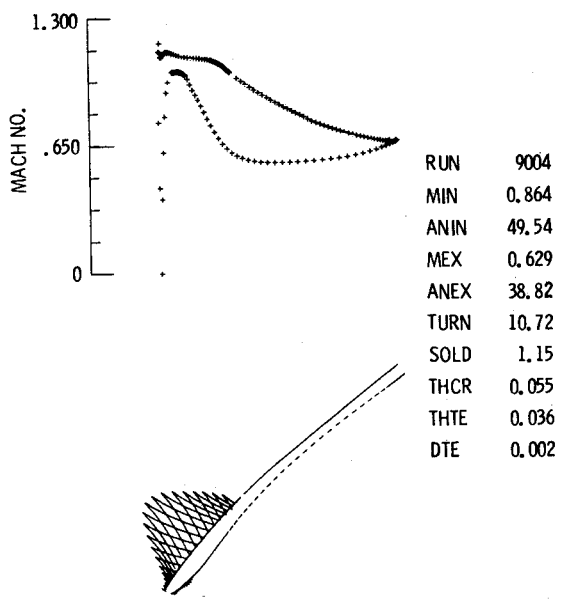

Fig. 4 Supercritical rotor section. Mach No. distribution.

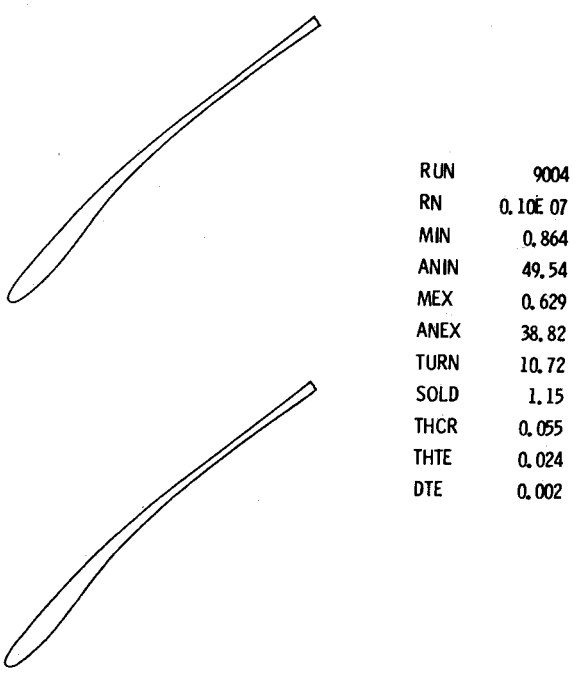

Fig. 5 Supercritical rotor section. Body shape.

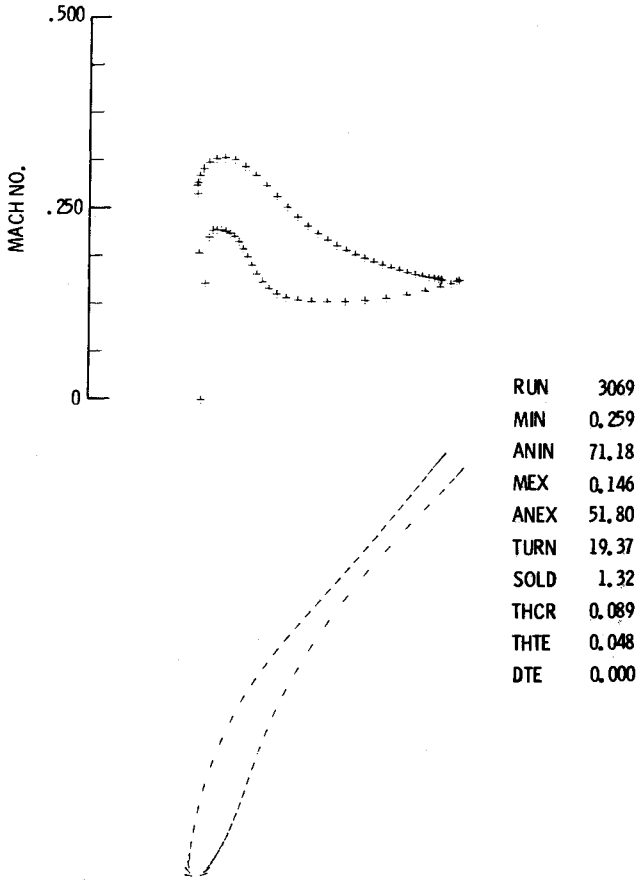

Fig. 6 High stagger subcritical rotor section. Mach No. distribution.

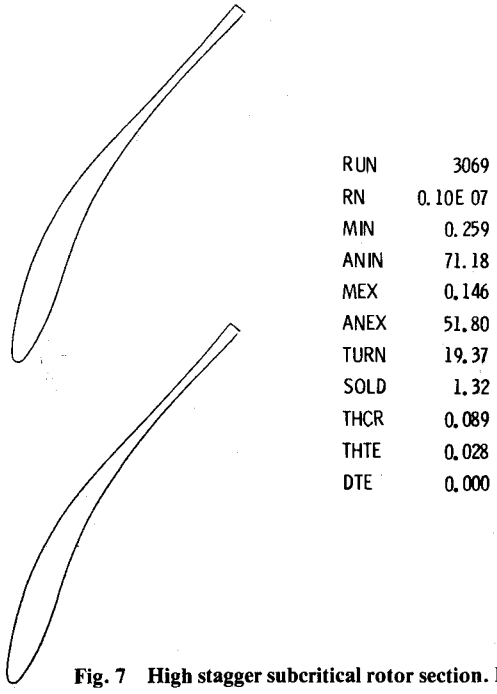

Fig. 7 High stagger subcritical rotor section. Body shape.

half of the blades are needed for a turbine rotor with this section, with the corresponding savings in weight and fabrication cost. The diffusion on the suction side is now considerably greater, but the reduction in the number of blades allows consideration of higher losses per blade with the same, or less, total loss.

The last example, Figs. 12 and 13, is a turning vane designed to operate at both zero incidence and 45 deg of

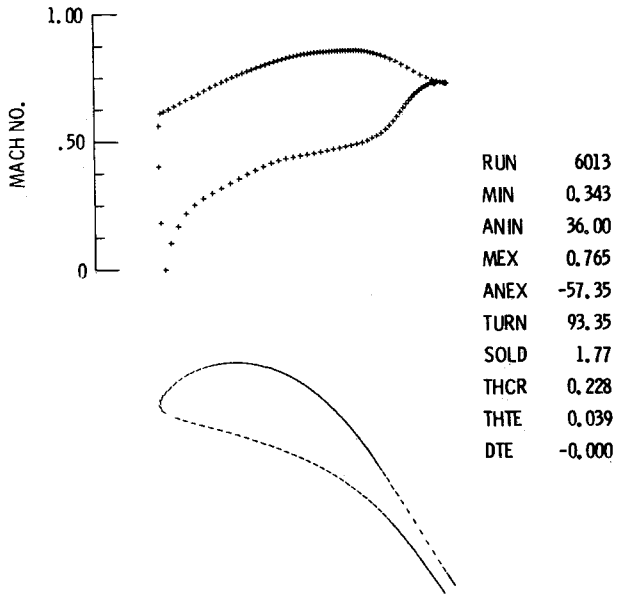

Fig. 8 Subcritical turbine blade. Mach No. distribution.

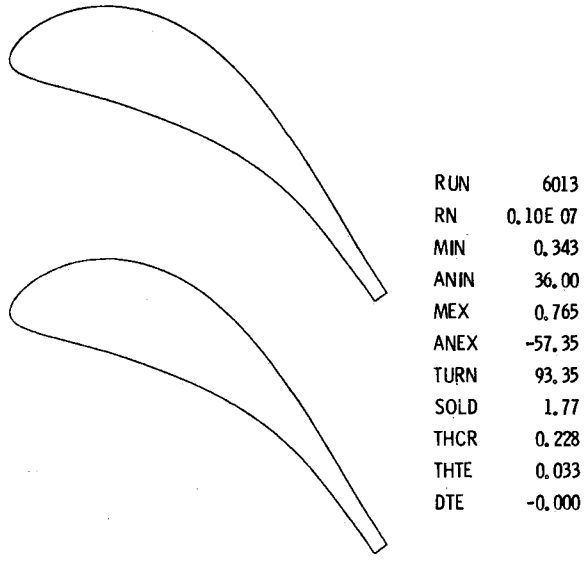

Fig. 9 Subcritical turbine blade. Body shape.

positive incidence, with the same exit flow angle in both modes of operation. Because of the blunt leading edge, large maximum thickness-to-chord ratio, and high solidity, this blade is capable of turning the flow for the 45 deg of the positive incidence operation mode.

The Mach number distributions in Figs. 2 and 4 present small "spikes" near the leading edge, which reflect the beginning of the formation of a limiting line. This is attributable to the high inlet Mach number of both designs. If it is considered that these "spikes" might trip the boundary layer, they would have to be eliminated by lowering the inlet Mach number.

IV. Boundary-Layer Correction

A turbulent boundary-layer computation has been incorporated into the inviscid inverse design code. We follow the lag-entrainment method as developed by Green et al.[3] This method contains less empirical factors than the classic of Nash and McDonald. It solves three ordinary differential equations for three independent parameters, the momentum thickness, the shape factor, and the entrainment coefficient, instead of one ordinary differential equation for the momentum thickness, as in Nash and McDonald.

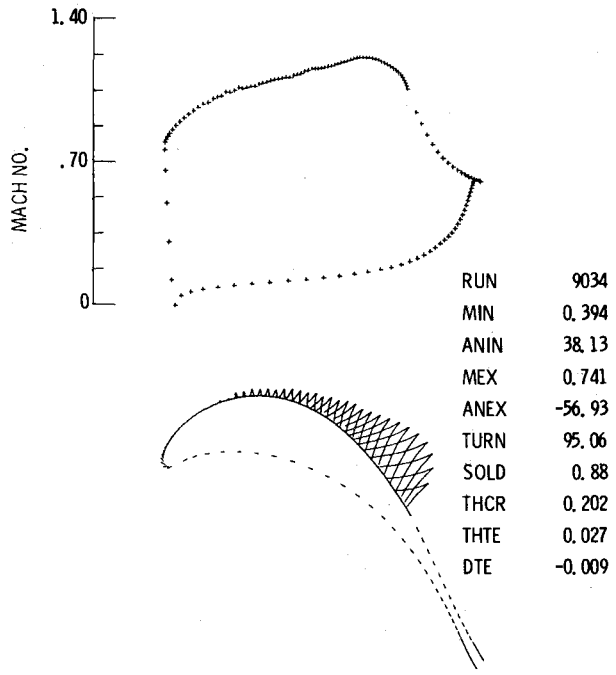

Fig. 10 Supercritical turbine blade. Mach No. distribution.

These three ordinary differential equations can be written as

$$\frac{d\theta}{ds} = \frac{C_f}{2} - (H+2-M^2)\frac{\theta}{q_e}\frac{dq_e}{ds}$$

$$\theta\frac{d\bar{H}}{ds} = \frac{d\bar{H}}{dH_1}\left[C_E - H_1\left\{\frac{C_f}{2} - (H+1)\frac{\theta}{q_e}\frac{dq_e}{ds}\right\}\right]$$

$$\theta\frac{dC_E}{ds} = F\left[\frac{2.8}{H+H_1}\left\{C_{\tau_{eq}}^{1/2} - \lambda C_\tau^{1/2}\right\} + \left(\frac{\theta}{q_e}\frac{dq_e}{ds}\right)_{eq} - \frac{\theta}{q_e}\frac{dq_e}{ds}\left\{1+f(M^2)\right\}\right] \quad (9)$$

where the three independent parameters θ, $\bar{H}$, and C_E are defined by

$$\theta = \int_0^\infty \frac{\rho q}{\rho q_e}\left(1-\frac{q}{q_e}\right)dy$$

$$\bar{H} = \frac{1}{\theta}\int_0^\infty \frac{\rho}{\rho_e}\left(1-\frac{q}{q_e}\right)dy$$

$$C_E = \frac{1}{\rho_e q_e}\frac{d}{ds}\left(\int_0^\delta \rho q dy\right) \quad (10)$$

The suffix e refers to flow variables at the edge of the boundary layer. The two other shape parameters and the skin friction coefficient are defined by

$$H = \delta^*/\theta$$

$$H_1 = \frac{1}{\theta}\int_0^\infty \frac{\rho q}{\rho_e q_e}dy$$

$$C_f = \frac{\tau_w}{\frac{1}{2}\rho_e {q_e}^2} \quad (11)$$

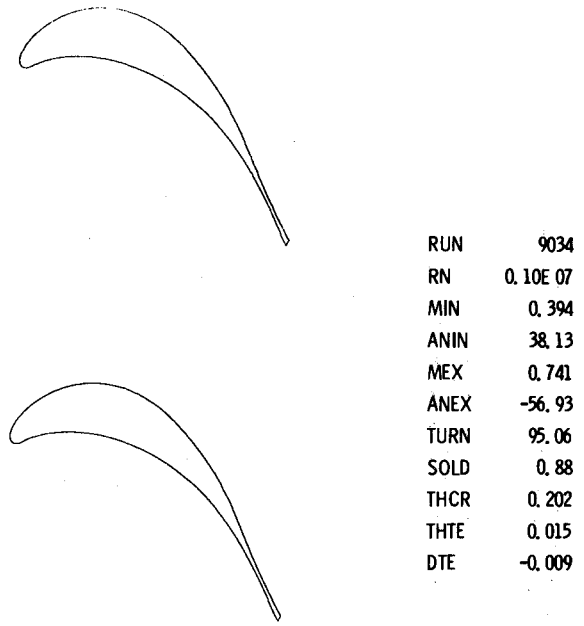

Fig. 11 Supercritical turbine blade. Body shape.

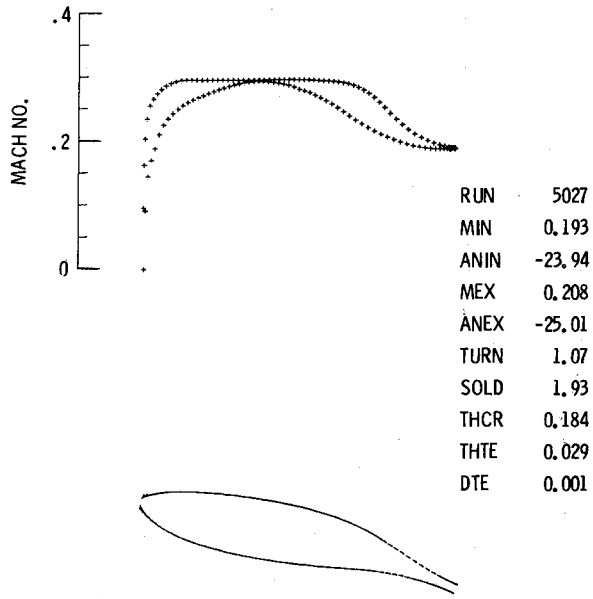

Fig. 12 Turning vane. Mach No. distribution.

See Ref. 3 for the definition and value of the other coefficients, which are functions of the entrainment coefficient and the local freestream magnitudes.

The transition point at which the computation of the boundary layer is started is left as an input parameter. Of the three initial values necessary to numerically solve the system of ordinary differential equations (9), only the initial momentum thickness is specified as an input parameter. The other two are computed by means of the equilibrium relations established in Ref. 3.

As described previously, once an inviscid airfoil has been obtained, the turbulent boundary-layer correction is switched on. The transition point is usually set at the point where the adverse pressure gradient starts. The Stratford criterion is followed to diffuse the flow from this point to the trailing edge. The Nash-McDonald separation parameter

$$\text{SEP} = -\frac{\theta}{q}\frac{dq}{ds} \quad (12)$$

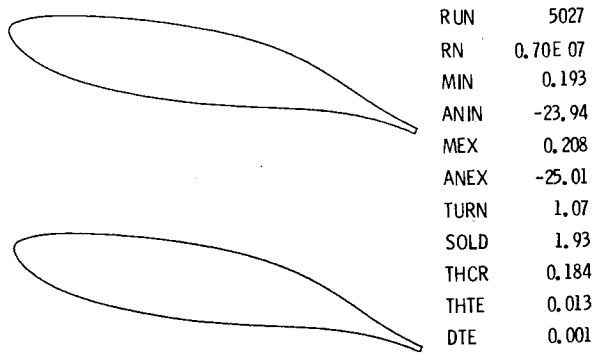

Fig. 13 Turning vane. Body shape.

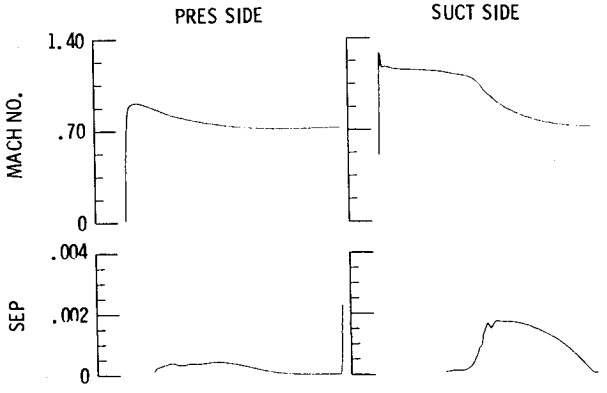

Fig. 14 Supercritical propeller section. SEP parameter.

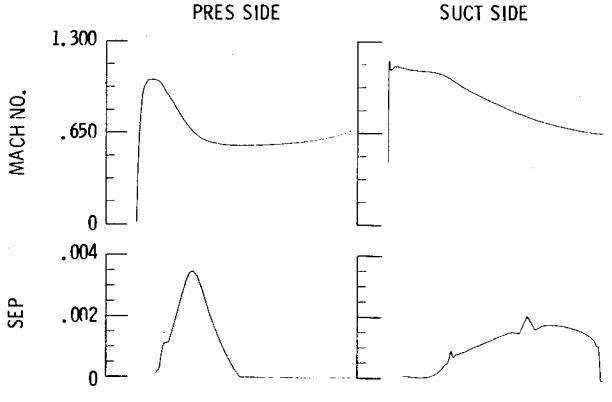

Fig. 15 Supercritical rotor section. SEP parameter.

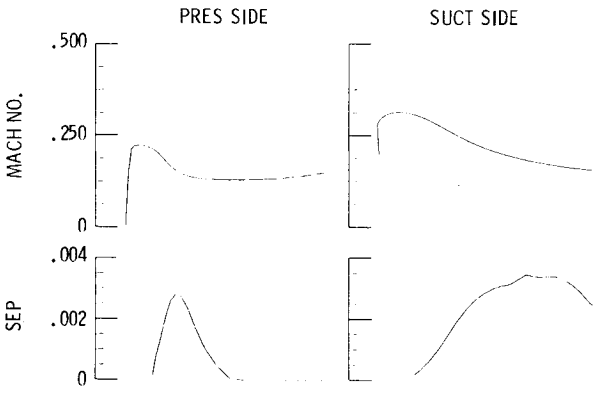

Fig. 16 High stagger subcritical rotor section. SEP parameter.

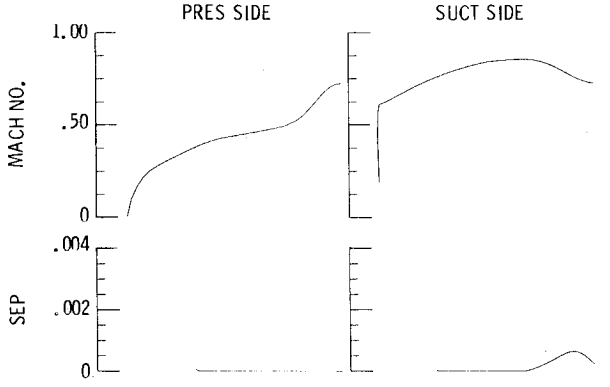

Fig. 17 Subcritical turbine blade. SEP parameter.

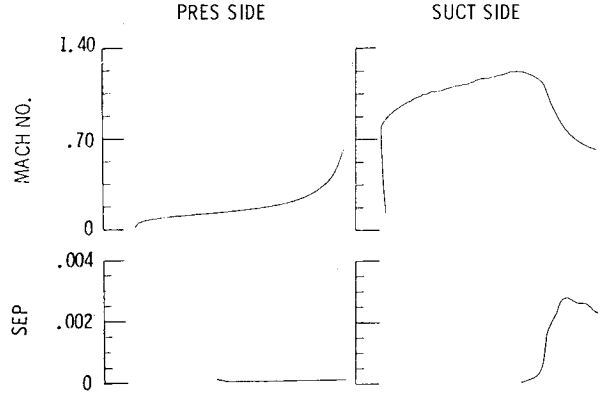

Fig. 18 Supercritical turbine blade. SEP parameter.

is used to predict separation. Separation is predicted when this parameter reaches a value of 0.004.

To achieve a nonseparated flow, the diffusion part of the input pressure distribution is modified, keeping the circulation constant until the desired value of the parameter SEP is reached. Each iteration produces a new airfoil with no significant change in the inlet flow conditions and solidity. Instead, the thickness at the trailing edge has to be monitored closely since it will determine the limits of the process. Figures 14-19 show the values of the parameter SEP for the six airfoils discussed in this paper. An initial Reynold number based on momentum thickness of 320 is assumed.

V. Elliptic Grid Generation

The elliptic transformation introduced in Ref. 2 to map the hodograph plane onto an ellipse can also be used to transform a cascade of airfoils in the physical plane onto an ellipse. Let z be a point in the physical plane of a cascade, and w the elliptic variable introduced in Sec. II. The domain of the variable w is the ellipse onto which the conformal transformation (3) maps the circular ring $1 < |\xi| < R$. Consider the conformal transformation defined by

$$\frac{dz}{dw} = -\frac{(w_T - w)^{1-\epsilon}}{w^2 - 1} \exp \sum_0^\infty c_n T_n(w) \tag{13}$$

with

$$w = \frac{1}{2}\left(\xi + \frac{1}{\xi}\right), \qquad 1 \le |\xi| \le R$$

and where $T_n(w)$ are the Tchebicheff polynomials defined in Sec. II.

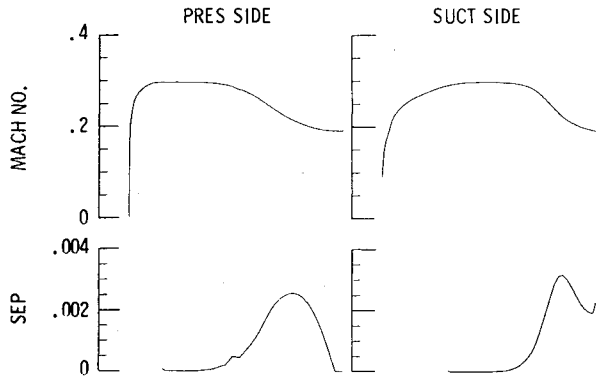

Fig. 19 Turning vane. SEP parameter.

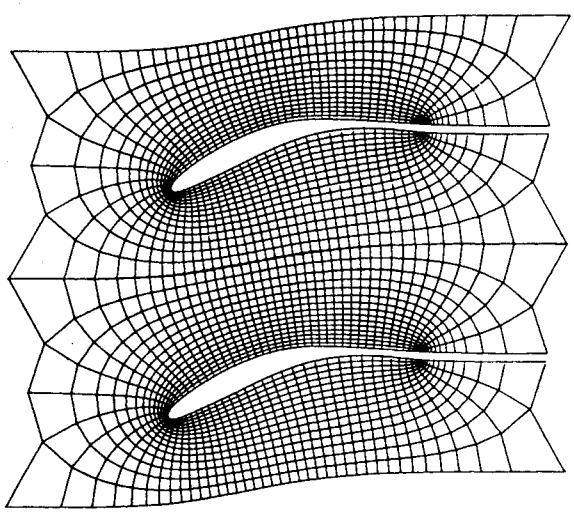

Fig. 20 Cascade grid for Korn airfoil.

This single transformation allows a cascade of airfoils with open trailing edge to be mapped onto the interior of the ellipse. The airfoil is mapped over the boundary and the trailing edge of the airfoil is transformed onto the point w_T. The upstream and downstream points of infinity are mapped onto the foci of the ellipse $w=\pm 1$. The angle at the trailing edge is given by $\epsilon \cdot \pi$.

Transformation (13) can be performed efficiently using the fast Fourier transform with a well-known iteration procedure first described by Theodorsen and Garrick, Ives and Liutermoza,[4] and Bauer et al.[1] It will be enough to say here that the convergence of the iterative procedure is achieved by imposing, at each iteration, the trailing-edge gap condition

$$dx+idy=\pi i\left\{(w_T+1)\exp\sum_0^\infty c_n T_n(-1) - (w_T-1)\exp\sum_0^\infty c_n T_n(1)\right\} \tag{14}$$

where dx and dy are the trailing-edge openings in the x and y directions.

The solidity is controlled by the parameter R and the stagger angle by the location of w_T. A Newton iteration automatically changes these two parameters to obtain the input solidity and stagger angle. This transformation, as in the hodograph design cases shown previously, can be used for cascades with solidities up to two. A grid generated with this transformation is shown in Fig. 20 for the Korn airfoil.

Because of the equivalence established previously between the ellipse and the circular ring, this circular ring can be used in conjunction with this transformation in the computational domain to solve the potential flow equations in an analysis mode.

VI. Conclusions

The new design code based on the method of complex characteristics and elliptic hodograph transformation is an efficient method for the design of airfoils in cascade. In particular, the design of subcritical cascades of airfoils is a very fast, robust, and versatile process. The inverse design code can be made to interact with a turbulent boundary-layer calculation to obtain airfoils with no separated flows at the design condition. The elliptic conformal mapping also can be used to generate grids for airfoils in cascade with open trailing edges.

References

[1] Bauer, F., Garabedian, P.R., and Korn, D., *Supercritical Wing Section I, II, III,* Springer-Verlag, Berlin, 1972, 1975, 1977.

[2] Sanz, J., "Design of Supercritical Cascades with High Solidity," AIAA Paper 82-0954, June 1982.

[3] Green, J. E., Weeks, D. J., and Brooman, W. F., "Prediction of Turbulent Boundary Layers and Wakes in Compressible Flow by a Lag-Entrainment Method," ARC-R/M-3791, RAE-TR-72231, 1977.

[4] Ives, D. C. and Liutermoza, J.F., "Analysis of Transonic Cascade Flow Using Conformal Mapping and Relaxation Techniques," AIAA Paper 76-370, July 1976.